Proc. Natl. Acad. Sci. USA
Vol. 93, pp. 4730–4735, May 1996
Cell Biology

Mos/mitogen-activated protein kinase can induce early meiotic phenotypes in the absence of maturation-promoting factor: A novel system for analyzing spindle formation during meiosis I

TAESAENG CHOI†, SHEN RULONG†, JAMES RESAU†, KENJI FUKASAWA†, WAYNE MATTEN†, RYOKO KURIYAMA‡, SAM MANSOUR§, NATALIE AHN§, AND GEORGE F. VANDE WOUDE†

†ABL–Basic Research Program, National Cancer Institute–Frederick Cancer Research & Development Center, P.O. Box B, Frederick, MD 21702; ‡Department of Cell Biology and Neuroanatomy, University of Minnesota Medical School, Minneapolis, MN 55455; and §Department of Chemistry and Biochemistry CB #215, University of Colorado, Boulder, CO 80309

Contributed by George F. Vande Woude, November 27, 1995

ABSTRACT **Mitogen-activated protein kinase (MAPK) is selectively activated by injecting either *mos* or MAPK kinase (*mek*) RNA into immature mouse oocytes maintained in the phosphodiesterase inhibitor 3-isobutyl-1-methylxanthine (IBMX). IBMX arrests oocyte maturation, but Mos (or MEK) overexpression overrides this block. Under these conditions, meiosis I is significantly prolonged, and MAPK becomes fully activated in the absence of $p34^{cdc2}$ kinase or maturation-promoting factor. In these oocytes, large openings form in the germinal vesicle adjacent to condensing chromatin, and microtubule arrays, which stain for both MAPK and centrosomal proteins, nucleate from these regions. Maturation-promoting factor activation occurs later, concomitant with germinal vesicle breakdown, the contraction of the microtubule arrays into a precursor of the spindle, and the redistribution of the centrosomal proteins into the newly forming spindle poles. These studies define important new functions for the Mos/MAPK cascade in mouse oocyte maturation and, under these conditions, reveal novel detail of the early stages of oocyte meiosis I.**

From invertebrates to mammals, mitogen-activated protein kinase (MAPK) is specifically activated during M phase in oocytes undergoing meiotic maturation (1–6), whereas little or no MAPK activation occurs during mitosis (5, 7, 8). The meiotic function of MAPK, however, is poorly understood. Gotoh *et al.* (9) showed that MAPK can induce the interphase–metaphase transition of microtubule (MT) arrays in *Xenopus* oocyte extracts. MAPK is a component of cytostatic factor (10) and induces *in vitro* cytostatic factor-like arrest (11). In mouse oocytes, MAPK localizes to MT organizing centers and to the meiotic spindle (6).

Mos is a serine/threonine protein kinase that, in *Xenopus*, is an initiator of oocyte maturation and an active component of cytostatic factor (12–14), as well as a potent activator of MAPK kinase (MEK) (15–17). Both the injection of Mos into fully grown oocytes (15) and the addition of Mos to *Xenopus* oocyte extracts (16) result in the rapid activation of MAPK. Thus, during oocyte maturation, certain downstream functions of Mos are very likely mediated by the MAPK cascade.

The investigation of MAPK functions during oocyte maturation independent of maturation-promoting factor (MPF) has not been possible, because, in *Xenopus*, MPF and MAPK have been considered to be in the same signaling pathway and are activated at approximately the same time (1, 9, 18). However, Matten *et al.* (19) demonstrated that Mos-induced MPF activation in *Xenopus* can be preferentially blocked by protein kinase A, under conditions where MAPK activation is unaffected. Here, we show that, as in *Xenopus*, MAPK can be activated in mouse oocytes in the absence of MPF, which permits an analysis of the influence of the Mos/MAPK cascade in oocyte maturation.

The phosphodiesterase inhibitor 3-isobutyl-1-methylxanthine (IBMX) inhibits mouse oocyte maturation by preventing cAMP breakdown, thereby maintaining intra-oocyte protein kinase A activity (20). We demonstrate that injection of RNA encoding either Mos or a constitutively activated form of MEK (MEK*) overrides the IBMX block to meiotic maturation. Under these conditions, at 12 hr after injection, MPF remains inactive, whereas MAPK is fully activated. In these oocytes, we observe large openings in the envelope of the germinal vesicle (GV), partial chromosome condensation, and the formation of MT arrays in and around the GV. MPF becomes activated at a later time and the oocytes complete maturation, becoming arrested at metaphase II. These studies identify new activities of the Mos/MAPK cascade and, because meiosis I is prolonged 12 hr, these experimental conditions provide a novel way to study the early stages of meiotic spindle formation.

MATERIALS AND METHODS

Oocyte Collection, Culture, and Microinjection. B6C3 F_1 female mice were injected intraperitoneally with 5 units of pregnant mare serum gonadotropin. Cumulus-enclosed oocytes were isolated 45–48 hr later and cultured in modified Whitten's medium (21) containing 0.4% BSA and 100 μM IBMX. For microinjection, oocytes were transferred to modified Whitten's media with Hepes (PGC Scientific, Gaithersburg, MD; specialty media) containing 5% fetal calf serum and 100 μM IBMX. Oocytes were injected in the cytoplasm with ≈10 pl of RNA (1 μg/μl) in Dulbecco's PBS. Injected or uninjected oocytes were washed in modified Whitten's medium containing IBMX and incubated at 38.5°C in humidified 5% CO_2 in air.

RNA was synthesized *in vitro* from the *mos*-containing plasmid, PHTX, with T7 RNA polymerase and the RNA cap analog, 7-methyl-G(5′)ppp(5′)G (22). Gain-of-function *mek** RNA (17) was synthesized *in vitro* using the same method. The RNA was precipitated twice in ethanol, then resuspended in Dulbecco's PBS.

Immunofluorescence and Confocal Microscopic Analysis. Oocytes were stripped of their zonae pellucidae with acidic Tyrode's solution (pH 2.5), fixed with 1.8% paraformaldehyde in PBS (fixing solution) for 40 min at room temperature, and made permeable with 1% Triton X-100 in fixing solution for 40 min. Oocytes were washed with 0.1% Tween-20 in PBS for 20 min and incubated with 3% BSA, 10% goat serum, and

The publication costs of this article were defrayed in part by page charge payment. This article must therefore be hereby marked "*advertisement*" in accordance with 18 U.S C. §1734 solely to indicate this fact.

Abbreviations: MAPK, mitogen-activated protein kinase; MT, microtubule; MEK, MAPK kinase; MPF, maturation-promoting factor; IBMX, 3-isobutyl-1-methylxanthine; GV, germinal vesicle; DAPI, 4′,6-diamino-2-phenylindol; GVBD, GV breakdown.

0.1% Tween-20 in PBS (blocking solution) for 1 hr at room temperature. Oocytes were then allowed to react with anti-tubulin antibody (YL½, Accurate Chemicals) at a 1:40 dilution or with anti-MAPK (Zymed) and anti-lamin B_2 monoclonal antibodies (23) at a 1:100 dilution in blocking solution for 1 hr at 37°C, followed by three washes in blocking solution. We used human autoimmune serum 5051 (24) at a 1:50 dilution to stain for centrosomal protein. The samples were then incubated with fluorescein isothiocyanate- or rhodamine-conjugated secondary antibodies at a 1:40 or 1:100 dilution for 1 hr at 37°C. To stain chromatin, 4′,6-diamino-2-phenylindol (DAPI) (5 μg/ml in PBS) was used. Images were prepared using a Zeiss 310 confocal laser scanning microscope as described by Tsarfaty *et al.* (25).

To compare the expression of Mos product in *mos* RNA-injected and control maturing oocytes, oocytes were stained with the Mos-specific ZC75 antibody and fluorescein isothiocyanate secondary antibody (26), and relative staining intensity was estimated by confocal laser scanning microscope average pixel intensity using the OPTIMAS 3.1 image analysis program (Edmonds, WA).

Electron Microscopy. Oocytes were fixed in 4% paraformaldehyde and 2.5% glutaraldehyde in PBS (pH 7.4) for 2 hr and washed for at least 2 hr with four changes of PBS. Oocytes were postfixed in 1% osmium tetroxide in PBS for 1 hr, dehydrated in acetone series, and embedded in Epon 812. The sections were picked up in 200-mesh copper grids and stained with uranyl acetate and lead citrate. The sections were observed in a Phillips EM 410 transmission electron microscope.

Histone H1 and MAPK Kinase Activities. Ten oocytes were lysed by freezing and thawing in 10 μl of reaction buffer containing 50 mM Tris·HCl (pH 7.2), 1% Nonidet P-40, 5 mM EGTA, 15 mM $MgCl_2$, 2 μg of aprotinin per ml, 2 μg of leupeptin per ml, 1 μg of pepstatin per ml, 20 μg of phenylmethylsulfonyl fluoride per ml, and 10 μg of cAMP-dependent protein kinase inhibitor peptide per ml (27). The H1 kinase activity was determined in 10 μl of reaction buffer containing histone H1 (100 μg/ml, Boehringer Mannheim) and [γ-^{32}P]ATP (50 μM, Amersham). After 15 min at 30°C, an equal volume of 2× SDS sample buffer was added, and the sample was boiled for 5 min. Samples were resolved by SDS/12% PAGE, and radioactivity in histone H1 was measured by liquid scintillation counting.

The MAPK activity was estimated by an in-gel kinase assay using a myelin basic protein substrate essentially as described by Kameshita and Fujisawa (28). The lysates, prepared from 20 oocytes, were denatured with 50 mM Tris·HCl, pH 8.0/1% SDS/1 mM DTT/0.2 mM EDTA for 15 min at 37°C and resolved on 10% polyacrylamide gels containing 0.5 mg myelin basic protein per ml (Sigma). The radioactivity in the MAPK bands was measured by liquid scintillation counting.

Western Blots and Immunoprecipitation. Thirty oocytes were lysed in SDS sample buffer, and extracts were resolved on 10% polyacrylamide gels. Proteins were transferred to nitrocellulose and probed with p34^{cdc2} monoclonal anti-PSTAIR antibody (21). The bound antibody was identified by using the ECL detection kit (Amersham).

For immunoprecipitation, 50 oocytes were labeled for 2 hr with 500 μCi (1 Ci = 37 GBq) of [^{35}S]methionine (1000 Ci/mmol, Amersham) per ml of culture medium. Radiolabeled oocytes were washed three times with culture medium, transferred to RIPA buffer, and frozen at −70°C. Samples were thawed, immunoprecipitated with anti-cyclin B antibody (PharMingen), and electrophoresed on SDS/polyacrylamide gels.

RESULTS

MAPK Activation Induced by *mos* RNA Injection. In *Xenopus* oocytes, Mos overexpression in the presence of protein kinase A activates MAPK, but not MPF (19). We examined, in mouse oocytes maintained in IBMX, the effect of *mos* RNA injection on MAPK and histone H1 kinase activities as well as on GV breakdown (GVBD) and polar body extrusion (Table 1). As expected, oocytes cultured with IBMX failed to undergo GVBD, and neither MAPK nor histone H1 kinase was activated; whereas, when IBMX was removed, uninjected oocytes matured normally and their MAPK and histone H1 kinase activities were elevated at 7 hr and later (Table 1). Quite surprisingly, when *mos* RNA was injected and IBMX was removed, the oocytes also matured normally, indicating that Mos overexpression has no obvious effect on oocyte maturation (data not shown).

By contrast to these controls, in the *mos* RNA-injected oocytes maintained in IBMX (Table 1), MAPK was activated at 12 hr and as early as 5 hr (data not shown). MPF activity, however, was not detectable until 12 hr and was maximum by 24 hr. In these oocytes, GVBD occurred as early as ≈16 hr, metaphase I occurred by 24 hr, and maturation was complete by 36–48 hr. Under these conditions, ≈80% of the *mos* RNA-injected, IBMX-treated oocytes complete maturation and arrest at metaphase II. Thus, Mos product, which is elevated ≈5-fold over endogenous levels by the injection of *mos* RNA (data not shown), can override the IBMX block to maturation; however, the early stages of meiosis I through GVBD are prolonged (≈16 hr) and, most importantly, MAPK, but not MPF, is activated during the first 12 hr.

MPF Activation in the Presence of IBMX. To determine why activation of MPF occurred so late, we examined the electrophoretic mobility of p34^{cdc2} to determine the state of phosphorylation. At 12 and 24 hr after *mos* injection in the presence of IBMX, slower moving forms of p34^{cdc2} were observed (Fig. 1*A*), indicating that p34^{cdc2} remained phosphorylated in oocytes that matured in the presence of IBMX, even after MPF activation at 24 hr. To test whether newly synthesized cyclin B appears when MPF activation occurs in the presence of IBMX, oocytes were labeled for 2 hr at 12 or 24 hr with [^{35}S]methionine and extracts were immunoprecipitated with anti-cyclin B antibody. As shown in Fig. 1*B*, newly synthesized cyclin B is

Table 1. Effect of IBMX and *mos* RNA on oocyte maturation

	Hours in culture			
	7	12	24	48
100 μM IBMX*				
MAP kinase§	0	20	25	ND
H1 kinase§	0	10	10	ND
GVBD¶	0	0	0	0
Polar body extrusion¶	0	0	0	0
100 μM IBMX + 10 pg *mos* RNA†				
MAP kinase§	ND	100	80	ND
H1 kinase §	ND	<10	100	ND
GVBD¶	ND	0	90	90
Polar body extrusion¶	ND	0	10	80
Control‡				
MAP kinase§	95	ND	80	ND
H1 kinase§	95	ND	100	ND
GVBD¶	100	100	100	100
Polar body extrusion¶	0	95	95	95

ND, not determined.

*Immature oocytes cultured continuously in IBMX.

†Immature oocytes cultured continuously in IBMX were injected with *mos* RNA.

‡Immature oocytes were initially exposed to IBMX, then the IBMX was removed to permit oocyte maturation to proceed.

§Kinase activities presented as percentages of highest activity observed in the experiment. MAPK activity was measured using a myelin basic protein substrate.

¶GVBD and polar body extrusion presented as percentage of total number of oocytes in each treatment group.

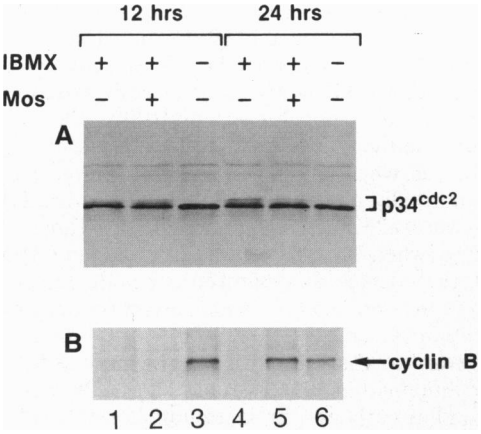

FIG. 1. Analyses of $p34^{cdc2}$ and cyclin B in maturing oocytes. (*A*) For $p34^{cdc2}$ Western blot analyses, extracts were prepared from *mos* RNA-injected IBMX-cultured oocytes at 12 hr (lanes 1–3) or 24 hr (lanes 4–6) and compared with extracts from control maturing oocytes using PSTAIR antibody. In the presence of IBMX, $p34^{cdc2}$ remains phosphorylated (lanes 1 and 4), even in oocytes injected with *mos* RNA (lanes 2 and 5). These oocytes, however, have high histone H1 kinase activity at 24 hr (Table 1) even though $p34^{cdc2}$ remains phosphorylated. Thirty oocytes were used per lane. (*B*) For cyclin B analyses, oocytes, cultured with or without IBMX and with or without *mos* RNA-injection, were labeled for 2 hr beginning at 12 hr and 24 hr. Immunoprecipitation of oocyte extracts was performed with anti-cyclin B antibody. In the presence of IBMX, cyclin B synthesis is detected in the *mos* RNA-injected oocytes at 24 hr.

present by 24 hr, but cyclin B synthesis can be detected as early as 16 hr (data not shown), the time at which MPF and GVBD are first observed. These data imply that the newly synthesized cyclin B could combine with dephosphorylated $p34^{cdc2}$ to trigger MPF activation.

Induction of MT Arrays by Mos and MEK* in the Absence of MPF. To determine whether the *mos* RNA-injected oocytes that exhibit high levels of MAPK activity in the absence of MPF were phenotypically different from oocytes maintained only in IBMX, we examined the state of MT assembly and chromosome condensation (Fig. 2). By confocal laser scan microscopy, uninjected oocytes maintained in IBMX showed tubulin and DAPI staining typical for a GV-arrested oocyte (Fig. 2 *a–c*). However, in the *mos*-injected oocytes maintained in IBMX, we observe MT arrays that appear to originate from within and around the swollen GV (Fig. 2 *d* and *g*) and partial chromosome condensation (Fig. 2 *e* and *h*) in the same scan. As revealed by computer overlay analysis (Fig. 2*i*), the MT arrays often colocalize with the regions of condensed chromatin. Two examples of *mos* RNA-injected oocytes at 12 hr show slight differences in MT array formation that we interpret to be earlier and later stages (Fig. 2 *d–f* and *g–i*, respectively).

To test more directly whether MAPK was implicated in the formation of GV MT arrays, we injected RNA encoding the activated form of MEK (MEK*) (17) into oocytes maintained in the presence of IBMX (Fig. 2 *j–l*). As with *mos* RNA-injected oocytes, 12 hr after *mek** RNA injection, the oocytes expressed high levels of MAPK activity (data not shown) without MPF activation. These oocytes also displayed GV MT arrays (Fig. 2*j*) and were indistinguishable from the *mos* RNA-injected oocytes (Fig. 2 *g–i*). Thus, in oocytes maintained in IBMX, both Mos and MEK* induce partial chromosome condensation and the formation of MT arrays and in the absence of MPF.

Location of MAPK and Lamin B in *mos* RNA-injected, IBMX-Treated Oocytes. MAPK localizes to the spindle and MT organizing centers in metaphase II-arrested oocytes (6); therefore, we examined whether MAPK was associated with the GV MT arrays in the absence of MPF. We found that

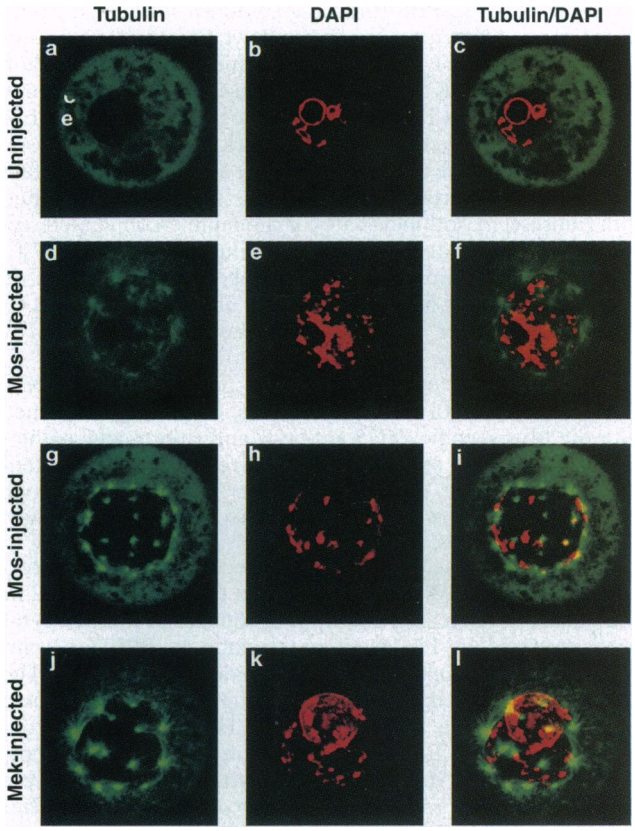

FIG. 2. Confocal laser scanning microscope analysis of *mos* or MEK* RNA-injected oocytes. Oocytes were stained with anti-tubulin YL½ antibody and DAPI. Uninjected control oocytes (*a–c*) show different cytoplasmic tubulin staining and some DAPI staining surrounding the nucleolus, but colocalization (tubulin and DAPI), indicated by yellow color in overlay analysis, is not observed. *mos* (*d–i*) or *mek** (*j–l*) RNA-injected oocytes incubated with IBMX for 12 hr displays large numbers of MT arrays in and around the GV. Partial chromosome condensation is also observed in the GV and, as revealed by the yellow color in overlay analysis, the areas of condensation are often associated with the MT arrays.

MAPK staining was diffuse in the cytoplasm of control oocytes maintained in IBMX (Fig. 3 *Upper c*), whereas in the *mos* RNA-injected oocytes, staining was especially intense in regions where the GV MT arrays were localized (Fig. 3 *Upper d*).

The nucleation of MTs from within the GV of the 12 hr *mos*- or *mek**-injected oocytes (Fig. 3 *Upper d*) would require changes in the GV membrane. Nuclear lamin is depolymerized during GVBD (29) and MAPK has been shown *in vitro* to phosphorylate lamin B on the same site phosphorylated by $p34^{cdc2}$ kinase that leads to the depolymerization of lamin B (30). We therefore examined the state of the nuclear lamin in the 12-hr *mos* RNA-injected oocytes. Control oocytes showed lamin B staining primarily in the region of the GV membrane (Fig. 3 *Upper a*), whereas oocytes stained 12 hr after *mos* RNA injection exhibited diffuse cytoplasmic lamin B staining and several regions in the GV membrane that were not stained, suggesting that the nuclear lamin might be partially depolymerized (Fig. 3 *Upper b*).

Consistent with this interpretation, electron microscopic examination of the GV membrane in the *mos* RNA-injected oocyte at 12 hr revealed large openings (≈200–800 nm) adjacent to the perinuclear electron-dense chromatin (Fig. 3 *Lower b*). Control oocytes lacked these areas of condensed chromatin and the GV membranes were intact (Fig. 3 *Lower a*). These large openings in the GV membrane are 10–20 times the size of nuclear pores and could readily allow exchange of GV and cytoplasmic components.

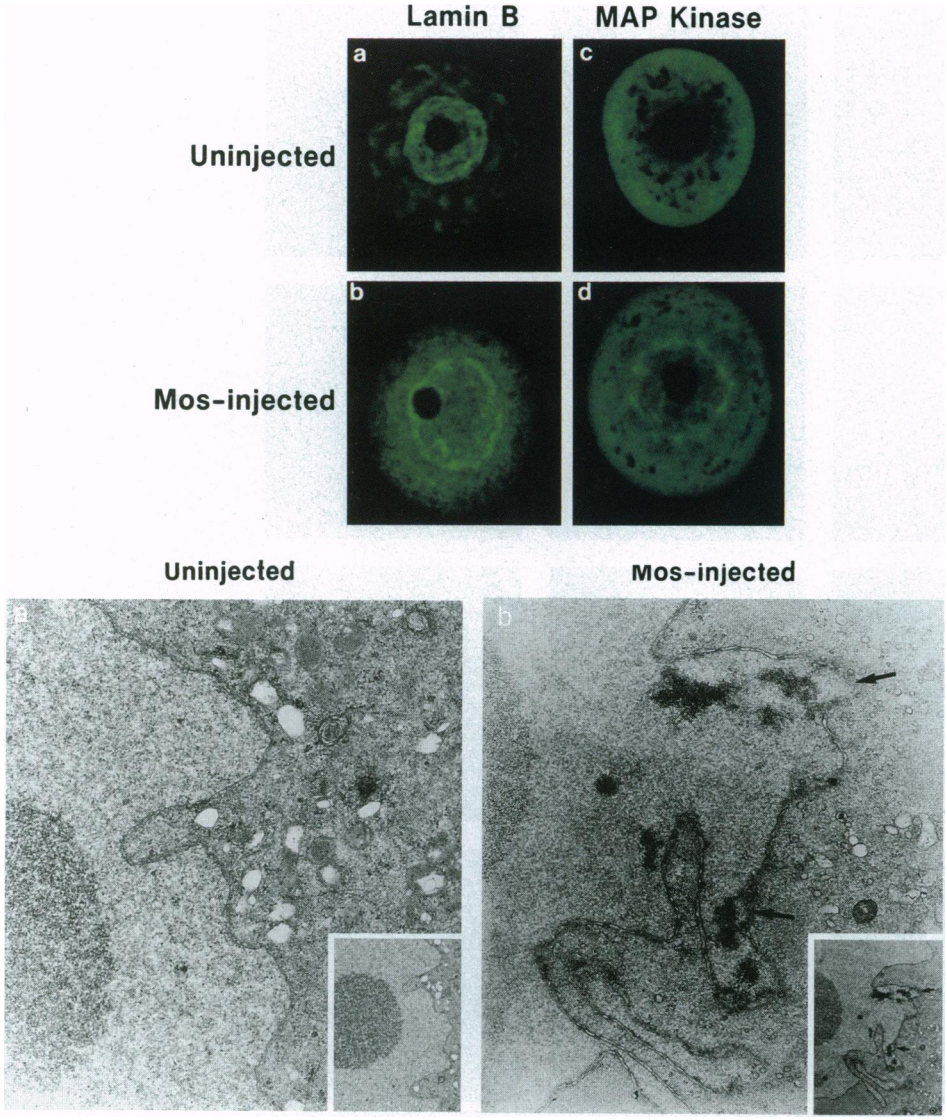

FIG. 3. Effect of MAPK activation on the integrity of the GV/nuclear membrane. (*Upper*) MAPK and nuclear lamin B localization in 12 hr *mos* RNA-injected oocytes. Oocytes were stained with anti-lamin B_2 antibody or anti-MAPK antibody. In *mos* RNA-injected, IBMX-treated oocytes examined at 12 hr, the lamin B staining was diffuse in the cytoplasm, which suggests that the nuclear lamin was partially depolymerized. MAPK staining was most intense in the MT arrays. (*Lower*) Electron micrograph analysis of the GV in *mos* RNA-injected oocytes. (*a*) Uninjected or (*b*) *mos* RNA-injected oocytes maintained in IBMX were examined at 12 hr after injection. Large openings (≈200–800 nM) were observed in the *mos* RNA-injected oocytes (arrows) in the GV adjacent to condensed chromatin.

Meiotic Spindle Formation. In the *mos* RNA-injected IBMX-treated oocytes, the formation of the first meiotic spindle occurs at 20–24 hr compared to 5–7 hr when IBMX is removed to allow maturation. This slower rate of spindle formation allowed us to study the details of the transition from the GV MT arrays at 12 hr to the meiotic spindle at 24 hr. To determine whether a meiotic spindle is formed under our special conditions, we stained oocytes 12–48 hr after *mos* injection with anti-tubulin antibody and DAPI, as well as with the human autoimmune serum 5051 (24) that recognizes the centrosomal protein pericentrin (31) (Fig. 4). Twelve hours after *mos* RNA-injection, all of the GV MT arrays have centrally localized pericentrin (Fig. 4 *a–c*). Moreover, the more punctate 5051 staining colocalizes with both DNA and the MT arrays and reveals a bivalent staining pattern (Fig. 4*c*, white arrows). Concomitant with MPF activation and GVBD at ≈16 hr, the centrosomal proteins aggregate and redistribute to the perimeter of the newly forming pre-spindle (Fig. 4 *d–f*) and subsequently move to the newly forming spindle poles (Fig. 4 *g*). In later stages of prometaphase (Fig. 4 *h–j*), as the first meiotic spindle elongates, the centrosomal proteins become more randomly distributed compared with their discrete location in the spindle poles of metaphase II-arrested oocytes (Fig. 4 *k* and *l*). Thus, the GV MT arrays induced by Mos/MAPK appear to be the precursors of the centrosome-containing spindle poles and first meiotic spindle.

DISCUSSION

To examine the specific role of MAPK in mouse oocyte maturation, we have employed a method to activate MAPK while MPF activation is delayed. We have shown that Mos/MAPK can induce the formation of multiple MT arrays, which appear to nucleate from condensing chromatin in and around the GV. Also, large holes develop in the GV, which are adjacent to condensed chromatin. By causing a substantial delay in GVBD and metaphase of meiosis I, our technique permits the detailed analysis of the early stages of meiosis I.

During mouse oocyte maturation, two types of centrosomal arrays were described by Messinger and Albertini (32). They found that cytoplasmic centrosomes are abundant after GVBD and exhibit a distinct pattern of appearance and disappearance during meiotic maturation. Under our conditions, we also observed cytoplasmic asters after GVBD and MPF activation, which implies that activated MPF is required for GVBD and cytoplasmic aster formation. By contrast, in *mos-* or *mek**-injected, IBMX-treated oocytes before MPF activation, only GV MT arrays are detected. These arrays could be related to the second type of centrosome that associates with the spindle and chromosomes (32).

Lamin B is phosphorylated and depolymerized during GVBD (29). *In vivo* chicken lamin B is phosphorylated on Ser-16, and *in vitro* $p34^{cdc2}$ kinase phosphorylates this serine, which induces the disassembly of nuclear lamin (33). Peter *et*

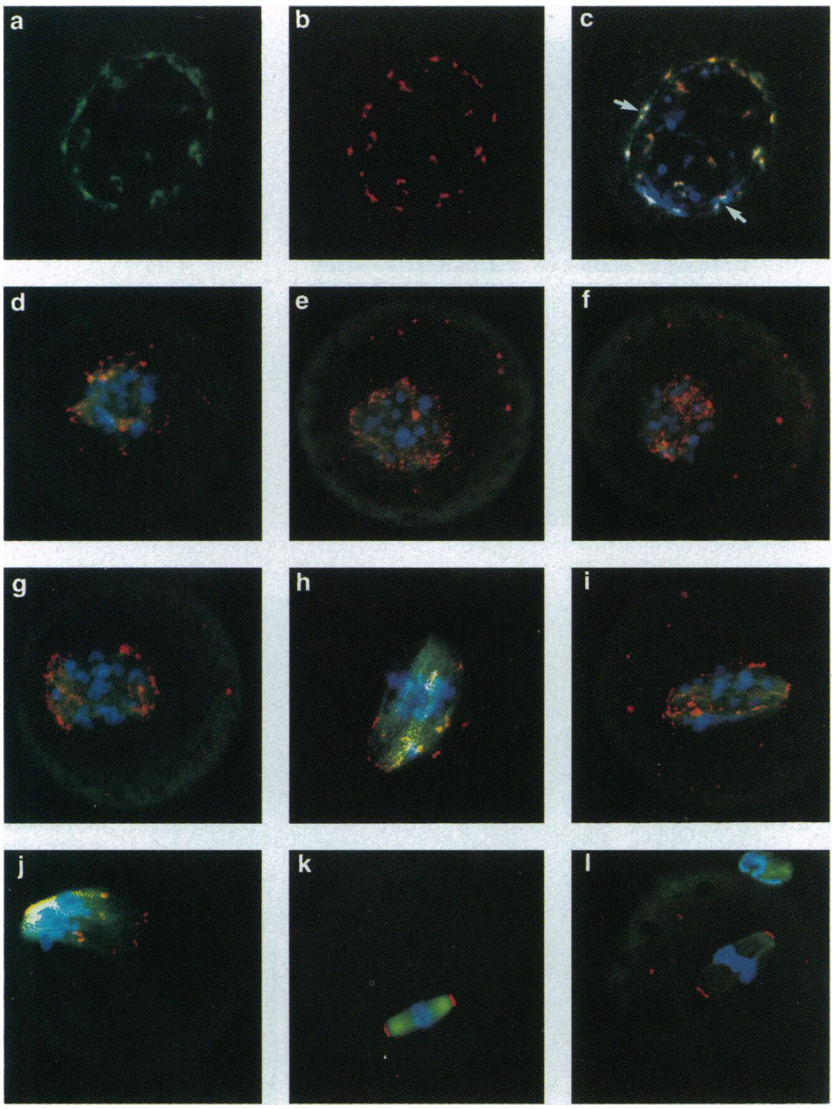

FIG. 4. Stages of meiotic spindle formation. Oocytes maintained in IBMX were selected at 12 to 48 hr after *mos* RNA-injection. Each panel shows a representative oocyte from each time point stained for tubulin (anti-tubulin antibody YL½), centrosomes (5051 antibody) and DNA (DAPI). The first three panels show tubulin (*a*), 5051 (*b*), and overlay analyses with DNA staining (*c*). The remaining panels (*d–l*) are the overlay analysis of representative oocyte examined at 16 hr (*d–f*), 18 hr (*g*), 20 hr (*h–j*), and 36–48 hr (*k–l*). At 12 hr the centrosomal staining is directly localized with the MT arrays and often colocalizes with condensed chromatin. The 5051 staining is more punctuate and in several cases (white arrows) the staining reveals a bivalent pattern. After MPF activation and GVBD, the 5051 staining redistributes to perimeter of the "pre-spindle" and is less colocalized with tubulin. At 18 hr (*g*) early stage of spindle pole formation shows 5051 staining is preferentially localized to emerging spindle poles. At 20 hr we show three examples of the first meiotic spindle at prometaphase and metaphase. The 5051 staining is still concentrated in the region of the spindle poles, but appears to be more scattered over the spindle than at 18 hr. At 36–48 hr 5051 staining in the metaphase II stage (*k* and *l*) is located either in the spindle pole region or in the cytoplasm as previously reported (32).

al. (30) have shown that MAPK also phosphorylates Ser-16 and induces nuclear lamin disassembly, but this disassembly is less efficient than that induced by $p34^{cdc2}$ kinase. Thus, the MAPK localized in the GV MT arrays (Fig. 3 *Lower*) may affect the localized dissolution of nuclear lamin, contributing to the formation of the large openings in the GV. Moreover, a recent study has shown that MAPK, rather than $p34^{cdc2}$ kinase, can induce GVBD in competent mouse oocytes treated with okadaic acid (34).

Xenopus oocytes require *de novo* protein synthesis for $p34^{cdc2}$ kinase activation before GVBD (35), whereas mouse oocytes only require protein synthesis for $p34^{cdc2}$ kinase activation after GVBD (36). Because cyclin B synthesis in mouse oocytes begins after GVBD and continues until metaphase II, previous studies suggested that cyclin B synthesis could be dependent on GVBD (37, 38). Our studies support this model, if in the absence of GVBD, the "large GV openings" induced by Mos/MAPK allow the release of an essential factor or factors required for cyclin B synthesis and MPF activation.

Our results suggest that activation of the Mos/MAPK cascade leads to partial chromosome condensation and the formation of novel GV MT arrays or "centrosomes." This result is consistent with the proposed role for MAPK in maintaining chromosomes in the condensed state and for preventing the formation of the nuclear envelope during meiotic interphase when MPF is depleted (8, 26). Mos/MAPK has previously been linked to a meiotic interphase function since, in *Xenopus*, inactivation of Mos during this period leads to reformation of the nucleus and the initiation of S-phase DNA synthesis (39).

Our analyses show that the MT arrays induced by Mos/MAPK form within the GV, because we can detect coincident chromatin, tubulin, and centrosomal protein staining. The frequent colocalization of the MT arrays with chromatin suggests that the condensed chromatin may participate in the nucleation of MT arrays. This observation is consistent with evidence showing that

oocyte meiotic spindle formation is chromosome-mediated (40) and serves to highlight one of the major differences between meiotic and mitotic spindle formation. In oocytes meiotic chromosomes have been shown to nucleate MTs. Dispersed chromatin, generated by nocodazol treatment of metaphase II-arrested oocytes, can nucleate MTs without association of MT organizing centers; later, however, MT organizing centers and chromosomes come together to form the spindle (40). Under our conditions, localized, rather than global, nuclear envelope disassembly occurs, and we can observe distinct stages of early meiosis I as Mos/MEK*/MAPK activation generates large openings in the GV coincident with the formation of MT arrays, partial chromosome condensation, and apparent nucleation of centrosome in regions of condensed chromatin. The activation of $p34^{cdc2}$ kinase triggers GVBD, the complete condensation of chromosomes and contraction of the centrosomal MT arrays to form a pre-spindle. The similarity of this stage to the prometaphase spindle of meiosis I in *Drosophila* females is striking (41). First, the spindle assembles around the chromatin, rather than from well-defined centrosomes; and the *Drosophila* karyosome (42) is remarkably similar to the condensed chromosomes and pre-spindle structure we observe (Fig. 4). Second, the *Drosophila* spindle begins with rather diffuse poles, which form into well-defined poles as prometaphase proceeds. Similarly, in mouse oocytes, the spindle poles are ill-defined and only emerge at later stages during reorganization of the centrosomes (Fig. 4).

Our results indicate that the Mos/MEK/MAPK pathway participates in MT, chromosomal, and GV envelope changes essential for meiosis. However, because Mos/MAPK function is absent in oocytes from Mos-deficient mice, and these oocytes mature normally, albeit at a much lower frequency (refs. 43 and 44; T.C., unpublished observations), these activities are not qualitatively essential, and other factors are likely to be involved. Remarkably, the overexpression of Mos or MEK* in oocytes in the absence of IBMX causes no change in the rate of oocyte maturation and no obvious morphological alteration in the matured oocyte (data not shown). In sharp contrast, the expression of Mos or MEK* in somatic cells induces morphological transformation and tumorigenesis (17, 45). Furthermore, we have shown that somatic cells that overexpress Mos display phenotypes that can be attributed to the meiotic activities of Mos/MAPK (26). The expression of these oocyte-specific activities in somatic cells could be responsible for many of the phenotypes of transformed cells in which the MAPK pathway is constitutively activated.

We thank Drs. E. A. Nigg (Swiss Institute for Experimental Cancer Research) and M. Yamashita (Hokkaido University, Japan) for anti-lamin B_2 antibody and cdc2 (PSTAIR) antibody; Dr. N. Copeland (ABL-Basic Research Program, National Cancer Institute–Frederick Cancer Research & Development Center, Frederick, MD) for valuable review and helpful comments; and Cheri Rhoderick for preparing the manuscript. This research was sponsored in part by the National Cancer Institute, Department of Health and Human Services, under contract NO1-CO-46000 with ABL. Additional research funding was provided by the G. Harold and Leila Y. Mathers Charitable Foundation.

1. Ferrell, J., Wu, M., Gerhart, J. & Martin, G. (1991) *Mol. Cell. Biol.* **11,** 1965–1971.
2. Haccard, O., Jessus, C., Cayla, X., Goris, J., Merlevede, W. & Ozon, R. (1990) *Eur. J. Biochem.* **192,** 633–642.
3. Posada, J. & Cooper, J. A. (1992) *Science* **255,** 212–215.
4. Pelech, S. L. & Sanghera, J. S. (1992) *Science* **257,** 1355–1356.
5. Shibuya, E., Boulton, T. G., Cobb, M. H. & Ruderman, J. V. (1992) *EMBO J.* **11,** 3963–3975.
6. Verlhac, M.-H., Pennart, H. D., Maro, B., Cobb, M. H. & Clarke, H. J. (1993) *Dev. Biol.* **158,** 330–340.
7. Kosako, H., Gotoh, Y., Matsuda, S., Ishikawa, M. & Nishida, E. (1992) *EMBO J.* **11,** 2903–2908.
8. Verlhac, M.-H., Kubiak, J. Z., Clarke, H. J. & Maro, B. (1994) *Development (Cambridge, U.K.)* **120,** 1017–1025.
9. Gotoh, Y., Nishida, E., Matsuda, S., Shiina, N., Kosato, H., Shirokawa, K., Akiyama, T., Ohta, K. & Sakai, H. (1991) *Nature (London)* **349,** 251–254.
10. Haccard, O., Sarcevic, B., Lewellyn, A., Hartley, R., Roy, L., Izumi, T., Erikson, E. & Maller, J. L. (1993) *Science* **262,** 1262–1265.
11. Minshull, J., Sun, H., Tonks, N. K. & Murray, A. W. (1994) *Cell* **79,** 475–486.
12. Sagata, N., Oskarsson, M., Copeland, T., Brumbaugh, J. & Vande Woude, G. F. (1988) *Nature (London)* **335,** 519–525.
13. Sagata, N., Watanabe, N., Vande Woude, G. F. & Ikawa, Y. (1989) *Nature (London)* **342,** 512–518.
14. Yew, N., Mellini, M. L. & Vande Woude, G. F. (1992) *Nature (London)* **355,** 649–652.
15. Posada, J., Yew, N., Ahn, N. G., Vande Woude, G. F. & Cooper, J. A. (1993) *Mol. Cell. Biol.* **13,** 2546–2553.
16. Nebreda, A. & Hunt, T. (1993) *EMBO J.* **12,** 1979–1986.
17. Mansour, S. J., Matten, W. T., Hermann, A. S., Candia, J. M., Rong, S., Fukasawa, K., Vande Woude, G. F. & Ahn, N. G. (1994) *Science* **265,** 966–970.
18. Gotoh, Y., Moriyama, K., Matsuda, S., Okumura, E., Kishimoto, T., Kawasaki, H., Suzuki, K., Yahara, I., Sakai, H. & Nishida, E. (1991) *EMBO J.* **10,** 2661–2668.
19. Matten, W., Daar, I. & Vande Woude, G. F. (1994) *Mol. Cell. Biol.* **14,** 4419–4426.
20. Schultz, R. M., Montgomery, R. R. & Belanoff, J. R. (1983) *Dev. Biol.* **97,** 264–273.
21. Choi, T., Aoki, F., Mori, M., Yamashita, M., Nagahama, Y. & Kohmoto, K. (1991) *Development (Cambridge, U.K.)* **113,** 789–795.
22. Yew, N., Oskarsson, M., Daar, I., Blair, D. G. & Vande Woude, G. F. (1991) *Mol. Cell. Biol.* **11,** 604–610.
23. Lehner, C. F., Eppenberger, H. M., Fakam, S. & Nigg, E. A. (1986) *Exp. Cell Res.* **162,** 205–219.
24. Calarco-Gillam, P. D., Siebert, M. C., Hubble, R., Mitchison, T. & Kirschner, M. (1983) *Cell* **35,** 621–629.
25. Tsarfaty, I., Resau, J. H., Rulong, S., Keydar, I., Faletto, D. L. & Vande Woude, G. F. (1992) *Science* **257,** 1258–1261.
26. Fukasawa, K., Murakami, M. S., Blair, D. G., Kuriyama, R., Hunt, T., Fischinger, P. & Vande Woude, G. F. (1994) *Cell Growth Differ.* **5,** 1093–1103.
27. Choi, T., Aoki, F., Yamashita, M., Nagahama, Y. & Kohmoto, K. (1992) *Biomed. Res.* **13,** 423–427.
28. Kameshita, I. & Fujisawa, H. (1989) *Anal. Biochem.* **183,** 139–143.
29. Dessev, G., Iovcheva-Dessev, C., Bischoff, J. R., Beach, D. & Goldman, R. (1991) *J. Cell. Biol.* **112,** 523–533.
30. Peter, M., Sanghera, J. S., Pelech, S. L. & Nigg, E. A. (1992) *Eur. J. Biochem.* **205,** 287–294.
31. Doxsey, S. J., Stein, P., Evans, L., Catarco, P. D. & Kirshner, M. (1994) *Cell* **76,** 639–650.
32. Messinger, S. M. & Albertini, D. (1991) *J. Cell Sci.* **100,** 289–298.
33. Peter, M., Nakagawa, J., Doree, M., Lobbe, J. C. & Nigg, E. (1990) *Cell* **61,** 591–602.
34. Chesnel, F. & Eppig, J. (1995) *Biol. Reprod.* **52,** 895–902.
35. Gerhart, J. C., Wu, M. & Kirschner, M. W. (1984) *J. Cell Biol.* **98,** 1247–1255.
36. Hashimoto, N. & Kishimoto, T. (1988) *Dev. Biol.* **126,** 242–252.
37. Choi, T. (1992) Ph.D. Thesis (Tokyo Univ., Tokyo).
38. Hampl, A. & Eppig, J. (1995) *Mol. Reprod. Dev.* **40,** 9–15.
39. Furuno, N., Nishizawa, M., Okazaki, K., Tanaka, H., Iwashita, J., Nakajo, N., Ogawa, Y. & Sagata, N. (1994) *EMBO J.* **13,** 2399–2410.
40. Maro, B., Johnson, M. H., Webb, M. & Flach, G. (1986) *J. Embryol. Exp. Morph.* **92,** 11–23.
41. Theurkauf, W. E. & Hawley, R. S. (1992) *J. Cell Biol.* **116,** 1167–1180.
42. Hawley, R. S. & Theurkauf, W. E. (1993) *Trends Genet.* **9,** 310–316.
43. Colledge, W. H., Carlton, M. B. L., Udy, G. B. & Evans, M. J. (1994) *Nature (London)* **370,** 65–68.
44. Hashimoto, N., Watanabe, N., Furuta, Y., Tamemoto, H., Sagata, N., Yokoyama, M., Okazaki, K., Nagayoshi, M., Takeda, N., Ikawa, Y. & Aizawa, S. (1994) *Nature (London)* **370,** 68–71.
45. Cowley, S., Paterson, H., Kemp, P. & Marshall, C. J. (1994) *Cell* **77,** 841–852.